Teske, A., Lizarralde, D., Höfig, T.W., and the Expedition 385 Scientists
Proceedings of the International Ocean Discovery Program Volume 385
publications.iodp.org

Data report: hydrocarbon profiles of selected IODP Expedition 385 Guaymas Basin samples and comparison to shallow surficial push core samples from AT42-05[1]

Paraskevi Mara,[2] Andreas Teske,[3] and Virginia Edgcomb[2]

[1] Mara, P., Teske, A., and Edgcomb, V., 2024. Data report: hydrocarbon profiles of selected IODP Expedition 385 Guaymas Basin samples and comparison to shallow surficial push core samples from AT42-05. In Teske, A., Lizarralde, D., Höfig, T.W., and the Expedition 385 Scientists, Guaymas Basin Tectonics and Biosphere. Proceedings of the International Ocean Discovery Program, 385: College Station, TX (International Ocean Discovery Program). https://doi.org/10.14379/iodp.proc.385.205.2024
[2] Department of Geology and Geophysics, Woods Hole Oceanographic Institution, USA. Correspondence author: **vedgcomb@whoi.edu**
[3] Department of Earth, Marine, and Environmental Sciences, University of North Carolina at Chapel Hill, USA.

Contents

Keywords
International Ocean Discovery Program, IODP, *JOIDES Resolution*, Expedition 385, Guaymas Basin Tectonics and Biosphere, Site U1545, Site U1546, Site U1547, Site U1548, Site U1549, Site U1550, Site U1551, deep biosphere, microbial degradation, hydrothermal, pushcore, aliphatic, petroleum, aromatic, and polyaromatic hydrocarbons, *Alvin*

Supplementary material

References (RIS)

MS 385-205
Received 3 November 2023
Accepted 6 August 2024
Published 1 November 2024

Abstract

Sediment and pore water samples from all drill sites of International Ocean Discovery Program (IODP) Expedition 385 were analyzed quantitatively for aliphatic hydrocarbons, petroleum (C_9–C_{44}) hydrocarbons, and aromatic and polyaromatic compounds. All hydrocarbon classes showed concentration peaks in deep, hot sediments just above and below deeply buried sills (Sites U1545 and U1546), indicating that they were formed by thermal maturation of buried organic matter in the thermal aureole of sill intrusion and have, to a large extent, remained in situ. Plotting hydrocarbon concentrations against in situ temperature shows a pronounced increase in concentration between 65° and 80°C, the thermal limit of hydrocarbon-degrading microbial populations. A smaller hydrocarbon maximum is associated with surficial sediments: within the upper 4 m of the sediment column, the concentrations of total saturated hydrocarbons and of total petroleum hydrocarbons were almost always higher compared to the next sediment samples in downhole sequence, compatible with biogenic hydrocarbon input that reaches all drill sites in Guaymas Basin. The U-shaped hydrocarbon profiles suggest a biological filter that degrades surficial hydrocarbon input and deeply sourced hydrocarbons as soon as the temperature regime in gradually cooling, slowly accumulating sediments permits microbial activity.

1. Introduction

The Guaymas Basin in the Gulf of California is a young marginal rift basin characterized by active seafloor spreading and rapid deposition of photosynthetic biomass, in particular diatoms, from highly productive overlying waters, supplemented locally by terrigenous sedimentation from the Sonora margin (Calvert 1966; Schrader 1982). Organic-rich sediments of several hundred meters thickness cover the spreading centers of Guaymas Basin and alternate with extensive magma intrusions (doleritic sills) that are inserted laterally into the unconsolidated sediments (Einsele et al., 1980). Generally, the organic carbon content of approximately 3–4 wt% in surficial Guaymas Basin sediments (De la Lanza-Espino and Soto, 1999) is reduced, presumably by heterotrophic microbiological activity, to 1–2 wt% in a wide range of subsurface sediments (Rullkötter et al., 1982; Gilbert and Summerhayes, 1982; Simoneit and Bode, 1982). In contrast to nonsedimented spreading centers at mid-ocean ridges that favor focused magma emplacement at the axial valley, the sediments in Guaymas Basin act as a thermal blanket that creates a broader zone of magmatism extending along axial-parallel faults (Berndt et al., 2016) and laterally into the sedimented off-axis flanking regions (Lizarralde et al., 2011; Teske et al., 2019). Emplacement of hot sills indurates

the sediment layers above and below the sill and alters their organic carbon content by transforming buried organic carbon into hydrocarbons (Whelan and Hunt 1982). Depending on location and depth, these hydrocarbons can be mobilized by hydrothermal circulation (Gieskes et al., 1982; Kastner, 1982). Thus, Guaymas Basin provides a natural laboratory to explore the transformation of buried organic matter under high pressure and temperature into complex mixtures of gaseous and liquid hydrocarbons and their mobilization toward the upper sediments and the seafloor (Claypool and Kvenvolden, 1983; Simoneit, 1985, 1990).

Here we report compound-specific hydrocarbon concentrations for sediment samples and pore water samples from the Guaymas Basin deep subsurface, collected during International Ocean Discovery Program (IODP) Expedition 385 (Table **T1**). The goal of this data report is to provide quantitative hydrocarbon data for geochemical and microbiological follow-up studies in the Guaymas Basin deep subsurface biosphere. We provide an initial overview of some downhole trends of major hydrocarbon classes (total petroleum hydrocarbons, saturated hydrocarbons, and polyaromatic [≥2 rings] hydrocarbons).

2. Methods

Sediment and pore water samples from all drill sites (Table **T1**) were analyzed at Alpha Analytical (Mansfield, MA, USA) for fingerprinting diagnostic compounds (e.g., saturated hydrocarbons, polynuclear aromatic hydrocarbons [PAHs], and alkylated PAHs) using EPA Method 8015 (gas chromatography–flame ionization detection [GC-FID]; saturates) and a modified Method 8270D (gas chromatography–mass spectrometric detection [GC-MS]; PAHs), as detailed in Stout (2016).

Sediments used for pore water extraction were prepared in a nitrogen-filled glove bag and then squeezed under laboratory atmosphere. Quantitative analyses of sediment cakes by GC-FID and GC-MS yielded detailed information on the amount and distribution of saturated petroleum hydrocarbons (C_9–C_{44}) and 2- to 4-ring PAHs as well as alkylated PAHs (Tables **T2**, **T3**). Overall, these analyses revealed significant variations at the molecular level at different drill sites in Guaymas Basin and along sediment depths.

Table T1. Sediment and pore water samples used for hydrocarbon fingerprinting, Expedition 385. **Download table in CSV format.**

Table T2. Hydrocarbon fingerprinting results for sediment samples, Expedition 385. **Download table in CSV format.**

Table T3. Hydrocarbon fingerprinting results for pore water samples, Expedition 385. **Download table in CSV format.**

3. Hydrocarbon distribution and in situ temperature

When total petroleum hydrocarbons, saturated hydrocarbons, and polyaromatic (≥2 rings) hydrocarbons are plotted against in situ temperature, the general trend of increasing hydrocarbon concentrations with temperature shows a conspicuous concentration step between ~65° and 80°C (Figures **F1**, **F2**, **F3**). At temperatures below this limit, all samples show comparable hydrocarbon concentrations for total petroleum hydrocarbons (C_9–C_{44}) and for total saturated hydrocarbons. Interestingly, total polycyclic aromatics with at least 2 rings have a more complex pattern and occur at high concentrations already at more moderate temperatures (Figure **F3**).

The reduced hydrocarbon concentrations at less than 65°C at all sites can be understood as reflecting the balance between hydrocarbon input and microbial degradation, with the caveat that cell

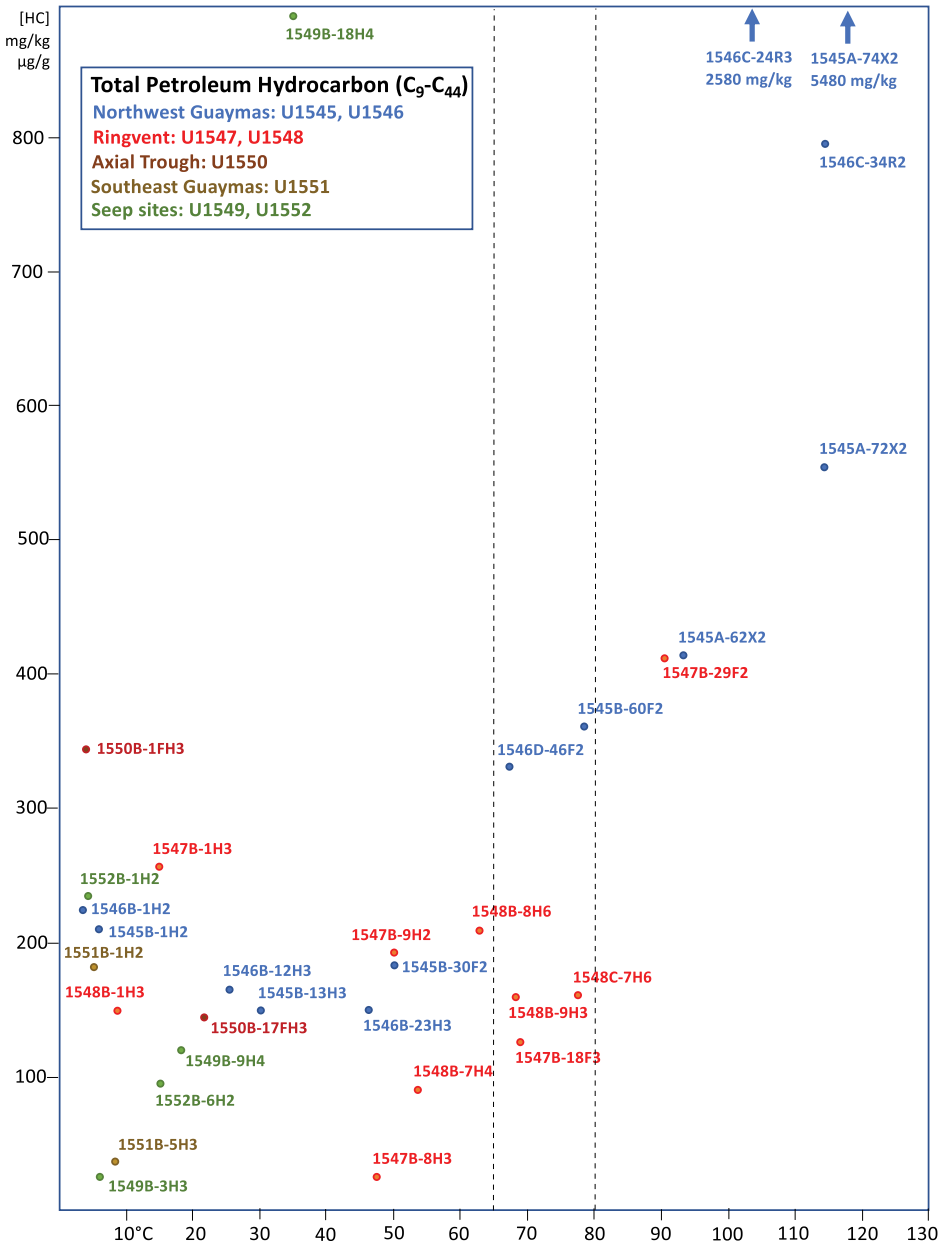

Figure F1. Total petroleum hydrocarbon [C_9–C_{44}] concentrations (mg/kg wet sediment) plotted against in situ temperatures (°C) for IODP Expedition 385 sediment samples (represented by hole and core section numbers). Dotted vertical lines mark the 65°–80°C transition from the microbial hydrocarbon-degrading temperature window into abiotic hydrocarbon generation.

abundance decreases steeply throughout the sediment column: from ~10^8 cells/cm^3 in shallow and cool sediments (~2.8° to 14.2°C) toward <10^2 cells/cm^3 in deep sediments at 65°C and higher temperatures (Morono et al., 2022). Hydrocarbon input would include localized petroleum sources at hydrothermal hotspots (Dalzell et al., 2021) but also ubiquitous sedimentary and microbial sources, such as plant-derived terrestrial hydrocarbon compounds (Rullkötter et al., 1982), phytoplanktonic hydrocarbon input (McGenity et al., 2021), autochthonous biomarkers produced by sediment bacteria and archaea (Mara et al., 2022), and in situ diagenetic production of recalcitrant compounds (Silliman et al., 1998). Accumulation would be checked by ubiquitous hydrocarbon-degrading microbial populations that—temperature permitting—are active across all drill sites. For example, the sulfate-reducing family Desulfatiglandales, a widespread lineage of mesophilic aromatics-remineralizing specialists in marine sediments (Teske, 2019), has been found in shallow subsurface sediments in and around Ringvent (Teske et al., 2019) and in surficial Guaymas Basin hydrothermal sediments (Ramirez et al., 2021; Edgcomb et al., 2022). Concerning alkane and

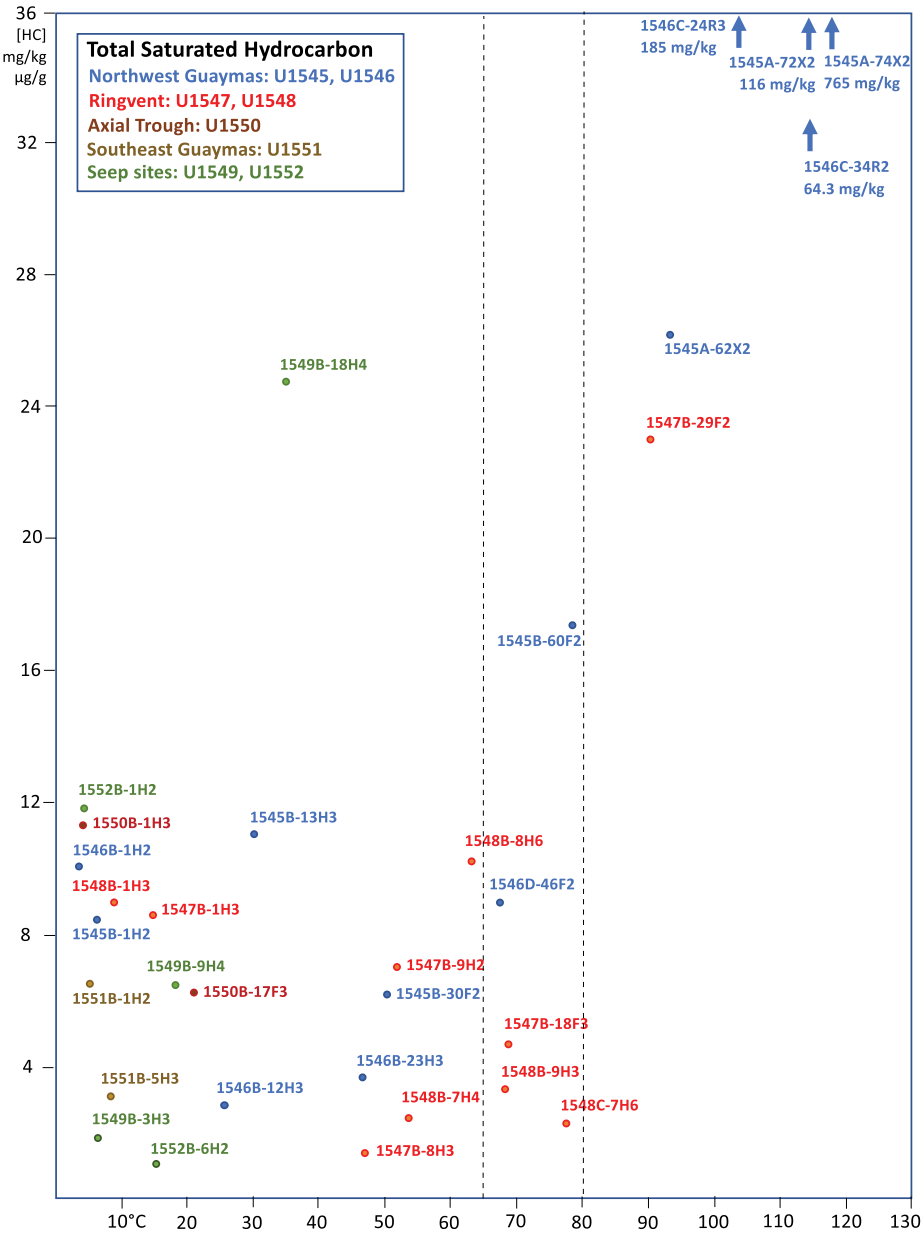

Figure F2. Total saturated hydrocarbon concentrations (mg/kg wet sediment) plotted against in situ temperatures (°C) for IODP Expedition 385 sediment samples (represented by hole and core section numbers). Dotted vertical lines mark the 65°–80°C transition from the microbial hydrocarbon-degrading temperature window into abiotic hydrocarbon generation.

petroleum degradation, laboratory experiments with Guaymas Basin enrichments from surficial sediments showed that light alkanes (C_6–C_{12}) and midlength alkanes (C_{16}–C_{18}) as well as crude oil are efficiently remineralized by mixed sulfate-reducing bacterial communities at 31° and at 55°C (Liang et al., 2023). The current thermal limits of hydrocarbon-degrading bacteria and archaea that have been studied in pure culture are near 70°–75°C for alkane-degrading consortia of sulfate-reducing bacteria (*Thermodesulfobacterium* spp.) and alkane-oxidizing archaea (*Alkanophaga* spp.) (Zehnle et al., 2023). The current thermal limit for methane-oxidizing bacterial/archaeal consortia enriched and isolated from hydrothermal sediments of Guaymas Basin is 70°C (Benito Merino et al., 2022).

At higher temperatures, microbial hydrocarbon utilization gradually decreases, as observed in hot petroleum reservoirs where microbial hydrocarbon processing stops between ~65° and 80°C (Head et al., 2003). For total C_9–C_{44} petroleum hydrocarbons and total saturated hydrocarbons, in

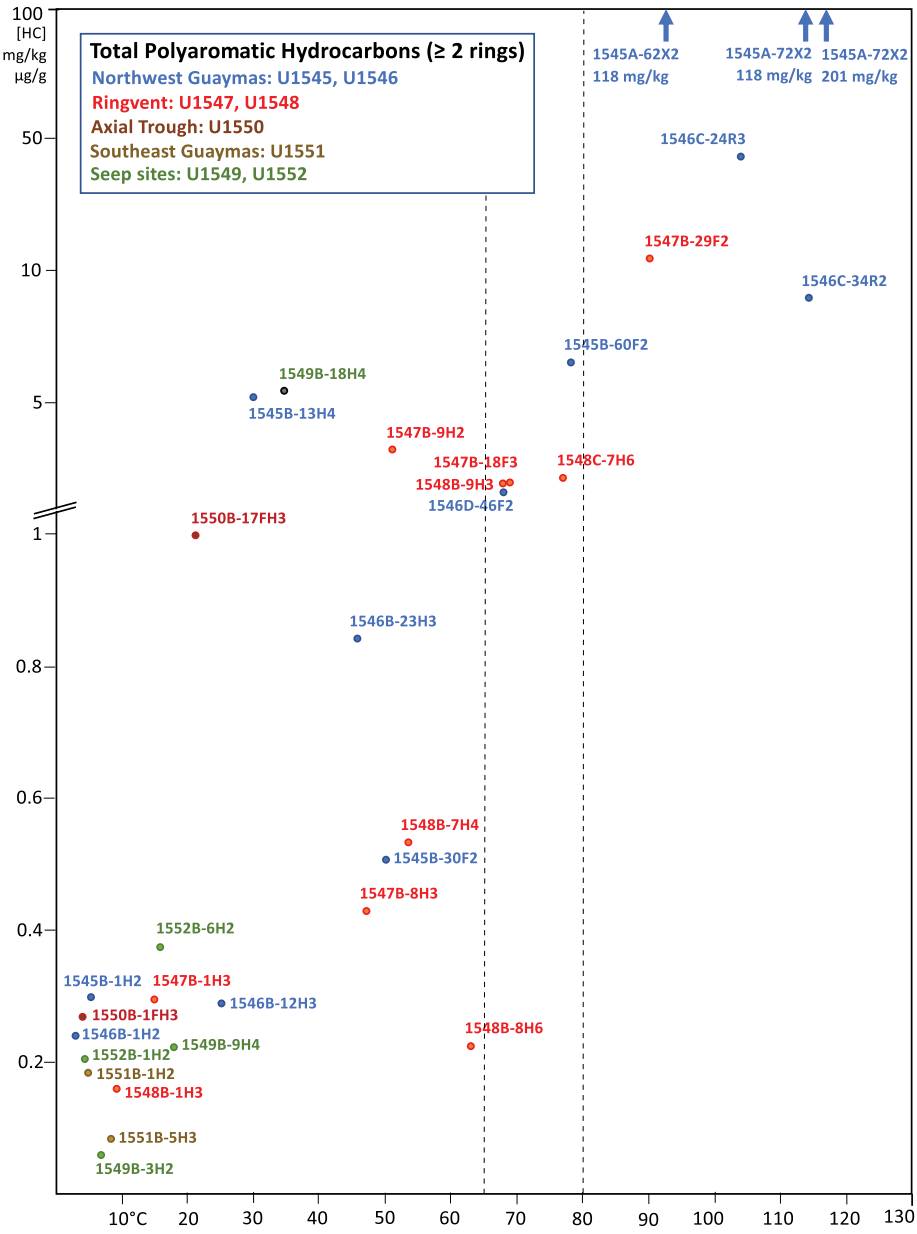

Figure F3. Total polycyclic aromatic [≥2 rings] hydrocarbon concentrations (mg/kg wet sediment) plotted against in situ temperatures (°C) for IODP Expedition 385 sediment samples (represented by hole and core section numbers). Note the changing y-scale > 1 mg/kg. Dotted vertical lines mark the 65°–80°C transition from the microbial hydrocarbon-degrading temperature window into abiotic hydrocarbon generation.

situ concentrations in Guaymas Basin sediments increased by an order of magnitude at temperatures of 100°C and higher. Because these temperatures inhibit microbial growth, microbial degradation is now prevented and instead hydrocarbons are formed by abiotic catagenesis from kerogen. Whereas total polycyclic aromatics with at least 2 rings showed highest concentrations above 65° and 80°C, their occurrence pattern was complicated by intermediate concentration peaks at more moderate temperatures (Figure **F3**).

3.1. Hydrocarbon accumulation at sills

The highest hydrocarbon concentration values were found in hot, indurated sediments immediately below sills (Table **T1**), indicating that the importance of in situ temperature is further modified by position relative to the sill: overlying sills cap the movement and hydrothermal mobilization of hydrocarbons, and they preserve hydrocarbon accumulations at sediment/sill contact zones. The sill intrusion at Site U1546 (between ~355 and ~432 m below seafloor [mbsf]) was emplaced at least 76,000 years ago (Lizarralde et al., 2023) and the even deeper sill intrusion at Site U1545 (near 482 mbsf) is probably older (**Teske et al.**, 2021a), yet both sill intrusions are accompanied by conspicuous hydrocarbon accumulations below them (Figures **F1**, **F2**, **F3**).

The sill-associated hydrocarbon peaks are consistent with rapidly decreasing methane/ethane ratios (trending toward 1:1) deeper than 485 mbsf at Site U1545 (**Teske et al.**, 2021a) and rapidly decreasing methane/ethane ratios (trending toward 40) just below the sill at Site U1546 (**Teske et al.**, 2021b). These anomalous methane/ethane ratios indicate the proximity of hydrocarbon reservoirs and forced termination of drilling at Sites U1545 and U1546 at 503 and 540 mbsf, respectively (**Teske et al.**, 2021a; **Teske et al.**, 2021b).

Hydrocarbon accumulation at sills was demonstrated during Deep Sea Drilling Project (DSDP) Leg 64 to Guaymas Basin, 40 years ago. In the hydrothermally active spreading center of Guaymas Basin at DSDP Site 477, the concentrations for a wide spectrum of saturated and aromatic compounds increased just below the shallow sill at this location by an order of magnitude compared to concentrations above the sill; these sill-associated peak concentrations also exceeded concentrations deeper down two- or threefold (Whelan and Hunt, 1982).

3.2. Surface hydrocarbon enrichment

In shallow sediments from the upper 4 m of the sediment column, the concentrations of total saturated hydrocarbons and of total petroleum hydrocarbons were almost always higher compared to the next sediment samples that follow in downward sequence (Table **T1**). The complete sample sequences from shallow to deep sediments, including hot samples taken from deeper intervals (Sites U1545/U1546 and Sites U1547/U1548), reveal a U-shaped concentration curve with local maxima in the upper sediment column followed by concentration minima at middepth, before increasing strongly in deep, hot sediments (Figure **F1**). This trend is visible for a wide spectrum of aliphatic compounds regardless of drill site (Table **T2**; see TableST2.xlsx in HYDROCARB in **Supplementary material**). This pattern might reflect planktonic sources—such as plant-derived alkanes (Rullkötter et al., 1982) or cyanobacterially produced alkanes (McGenity et al., 2021)—that increase the hydrocarbon content of surficial sediments everywhere in Guaymas Basin, independently of hydrothermal activity. We note that phytoplankton-derived biomarkers were found consistently in Guaymas Basin surficial sediments (Mara et al., 2022). As an alternative explanation, sill-associated hydrocarbons could migrate in the seabed and reach surficial sediments where they condense and precipitate under cool temperatures (Kawka and Simoneit, 1994). However, we note that this explanation is less likely at sites where hydrocarbon reservoirs are buried at several hundred meters depth with no obvious flow paths to the surface (Sites U1545 and U1546). We also note that temperature-induced hydrocarbon precipitation and condensation would not need to be limited to the upper 4 m, as cool temperatures often persist below this depth. In general, thermal mobilization and near-surface condensation of hydrocarbons would be most plausible at sites with shallow sills, for example DSDP Sites 477 and 478 (Kawka and Simoneit, 1994).

3.3. Polyaromatics (PAHs) occurrence patterns

In contrast, most polyaromatic compounds did not show this enrichment in the upper sediment column and subsequent minima at middepth; instead, they followed an initially very gradual downhole increase that became steeper with depth and temperature, finally leading toward maximal concentrations in deep, hot sediments (Table **T2**; see TableST2.xlsx in HYDROCARB in **Supplementary material**). The 2- to 4-ring PAHs in our sample collection of sediment cakes consisted mainly of the parent and alkylated isomers of naphthalene, fluorene, phenanthrene/anthracene, fluoranthene/pyrene, and chrysene.

In contrast to other polyaromatic compounds that were selectively enriched only near sill intrusions, the 5-ring compound perylene occurred at all sites in high concentrations (2–12 mg/kg sediment) throughout most of the deep sediment column, with lower concentrations limited to surficial samples and very deep sill samples. This distribution pattern changes the overall profile of PAH concentrations in the temperature plot and contributes to high total PAH concentrations in several deep subsurface samples below the 65°C threshold where microbial degradation takes place (Figure **F3**). Whereas potential origins of perylene include terrestrial soil fungi (Hanke et al., 2019), the accumulation of perylene in marine sediments without significant terrestrial input (Wakeham et al., 1979) suggests a marine planktonic source. For Guaymas Basin, abundant diatoms are a likely candidate (Venkatesan, 1988). Yet the reduced perylene concentrations in the upper sediment column argue against direct deposition as the only major source. Ubiquitous accumulation throughout the sediment column and basin-wide occurrence suggest in situ diagenetic production within the sediment column from a wide range of precursor materials (Silliman et al., 1998) and petrogenic sources (Kawka and Simoneit, 1994), combined with preservation of this recalcitrant compound within the temperature range of microbial degradation (<65°–80°C). Interestingly, perylene concentrations were strongly reduced in deep sediments near sill intrusions (Sites U1545–U1548), indicating that this ubiquitously accumulating and highly recalcitrant compound has decayed within the thermal aureole of sill emplacement. Because concentrations of other types of PAHs (phenanthrenes, anthracenes, pyrenes, and chrysenes) increase sharply in the same samples near sills, they should have been produced during sill emplacement (Table **T2**; see TableST2.xlsx in HYDROCARB in **Supplementary material**).

3.4. Outliers

In cool and temperate samples where microbial hydrocarbon degradation is not inhibited, polyaromatic concentrations were generally <0.5 µg/g wet sediment, saturated hydrocarbon concentrations were less than ~12 µg/g, and total petroleum hydrocarbon concentrations were less than 250 µg/g. The exception to this pattern is "cold seep" Section 385-U1549B-18H-4, sampled at 161 mbsf; this moderately heated sample (~35°C in situ temperature) contained more than 5 µg/g PAHs, ~25 µg/g saturated hydrocarbons, and nearly 900 µg/g total petroleum hydrocarbons, suggesting a deep hydrocarbon source that imprints unusually high concentrations into this temperate sediment sample. This sample was obtained just above the massively disturbed deep sediment layers that surround the "Octopus Mound" cold seep site (**Teske et al.**, 2021d). At this location and depth, drilling was terminated to avoid tapping a potential petroleum and gas reservoir (Teske et al., 2018). The co-occurrence of high petroleum hydrocarbon concentrations and moderately warm temperatures in deep, sulfate-depleted sediments suggests potential for microbiological studies, for example, enrichments for methanogenic alkane degraders (Ca. *Methanoliparia*; Laso-Pérez et al., 2019) that are so far missing in Guaymas Basin (Teske, 2024).

3.5. Pore water samples

Sediment pore waters contained aliphatic and aromatic hydrocarbons, including the same parent and alkylated isomer compounds as reported for sediment cakes, but due to low aqueous solubility they were present only at 2–3 orders of magnitude lower concentrations, on average, compared to sediment cakes (Tables **T1**, **T3**; see TableST3.xlsx in HYDROCARB in **Supplementary material**). Indurated sediments near sills did not yield pore water, and no data on pore water hydrocarbon content are available for these samples.

Most pore water samples had total petroleum hydrocarbon concentrations between 0.25 and 0.29 mg/kg, suggesting a consistent background in the sediment column across Guaymas Basin. Higher totals were found for samples obtained from Sections 385-U1548C-7H-6 (63.9 mbsf), 385-U1549B-3H-3 (17.4 mbsf), 385-U1549B-9H-4 (75.4 mbsf), and 385-U1550B-1H-3 (4.3 mbsf) (Table **T3**; see TableST3.xlsx in HYDROCARB in **Supplementary material**). These elevated totals suggest the influence of hydrocarbon migration from underneath the lip of the sill underlying Ringvent (Section 385-U1548C-7H-6, sampled at 63.9 mbsf, yielded the deepest and hottest pore water sample of the most proximal core to the hydrothermally active Ringvent structure) and hydrocarbon input from the Octopus Mountain seep area (Sections 385-U1549B-3H-3, 9H-4). Pore water sample from Section 385-U1551B-4H-3 (26.8 mbsf) stands out by 2–3 times elevated concentrations across the entire spectrum of aromatic and (to a lesser degree) aliphatic compounds (Table **T3**; see TableST3.xlsx in HYDROCARB in **Supplementary material**). The unusually coarse-grained lithology at this site and depth (diatom-bearing silty sand to clayey silt and local intervals of sulfide- or organic-rich clayey silt and silty sand) suggests terrestrial sedimentation and organic input at this site (**Teske et al.**, 2021e); the changing lithology might influence the partition between particle-bound and soluble hydrocarbons. Pore water concentrations for total PAH (≥2 rings) were generally near 5500 ng/L in most samples, with higher concentrations limited to the samples of Sections 385-U1545B-60F-2 (325.1 mbsf) and 385-U1551B-4H-3 (26.8 mbsf) (Table **T3**; see TableST3.xlsx in HYDROCARB in **Supplementary material**).

4. Comparison with hydrocarbons in surficial Guaymas Basin sediments

In 2018, we performed hydrocarbon profiling of surficial sediments (Mara et al., 2022) that were collected using human occupied vehicle (HOV) *Alvin*. Sediment pushcores were recovered at hydrothermally active areas in the southern axial trough of Guaymas Basin (maximum core length ~60 cm; recovered sediment length between 18 and 30 cm) (Tables **T4**, **T5**; see TableST5.xlsx in HYDROCARB in **Supplementary material**). Sediment and pore water samples were analyzed by GC-FID and GC-MS at Alpha Analytical (Mansfield, MA, USA) as described previously (Mara et al., 2022). Pore water extraction from these surficial samples was performed using centrifugation and is therefore not directly comparable to the more comprehensive shipboard pore water extraction by sediment squeezing during IODP Expedition 385. Thus, the distribution of hydrocarbons between pore water and sediment in these surficial samples favored the sediment phase for the pushcore samples. Consequently, pore waters in these more surficial sediment samples contain 3–4 orders of magnitude lower hydrocarbon concentrations than the sediment phase (Tables **T4**, **T5**; see TableST5.xlsx in HYDROCARB in **Supplementary material**). These caveats must be kept in mind when comparing surficial and deep sediment results (Table **T4** vs. Table **T1**).

PAH concentrations in surficial hydrothermal sediments (~10 to 350 mg/kg sediment) were similar to peak PAH concentrations in the deep, hot subsurface near sills (10–200 mg/kg sediment). Petroleum hydrocarbon (C_9–C_{44}) concentrations in surficial hydrothermal sediments (maximally 1,000–10,000 mg/kg sediment) were noticeably higher than in deep, hot sediments near sills (500–5,000 mg/kg sediment), suggesting that the *Alvin* pushcores had sampled a natural conduit that funneled concentrated petroleum hydrocarbons toward the sediment surface. Interestingly, total saturated hydrocarbon concentrations in surficial sediments (maximum 10–50 mg/kg, in one sample near 400 mg/kg sediment) were lower compared to those in deep, hot sediments near sills

Table T4. Sediment and pore water samples used for hydrocarbon fingerprinting using HOV *Alvin* pushcores during the AT42-05 cruise in Guaymas Basin in November 2018 (R/V *Atlantis*). **Download table in CSV format.**

Table T5. Hydrocarbon fingerprinting results for surficial hydrothermal sediments using HOV *Alvin* pushcores during the AT42-05 cruise in Guaymas Basin in November 2018 (R/V *Atlantis*). **Download table in CSV format.**

(maximally 100–800 mg/kg sediment), indicating increased retention of these compounds in the deep subsurface.

The hydrocarbon concentrations in surficial sediments suggest that hydrothermal activity affected the distribution of hydrocarbons at the different sampling sites (Mara et al., 2022). In warm sediments (Cathedral Hill area; 30°C at 20 cm below seafloor, cmbsf), total petroleum and total saturated hydrocarbons as well as polyaromatic compounds occurred at similar concentrations at all examined sediment horizons. In extremely hot sediments (Marker 14 area; >100°C at 30 cmbsf), these concentrations peaked in the uppermost sediment layer and declined by an order of magnitude downcore (Table **T4**), demonstrating the effect of hydrothermal mobilization that flushes hydrocarbons from deeper, hotter sediment layers and traps them in cool surficial sediments.

Generally, hydrocarbon seepage in hydrothermal hotspots of the southern Guaymas Basin differs in several aspects (depth and age of organic carbon source compounds) from the hydrocarbon accumulations at depth (i.e., in deep, hot sediments near emplaced sills). High-resolution bathymetric surveys combined with shallow subbottom seismic profiles penetrating ~30–60 m below the sediment surface in the southern axial trough of Guaymas Basin (Ondréas et al., 2018) showed that seepage is concentrated in small seafloor depressions harboring massive subsurface hydrothermal precipitates. Here, hydrothermal fluids follow relatively shallow and convoluted flow paths that skirt surface-breaching hydrothermal edifices and finally emerge at their sedimented base or on the talus slope where these fluids sustain hydrothermal hotspots and microbial mats (Dowell et al., 2016). The hydrothermally active zone in the southern axial trough of Guaymas Basin is most likely fueled by shallow sills, similar to the massive sill encountered in DSDP Holes 477 (58–105 mbsf) and 477A (32.5–62.5 mbsf) (Shipboard Scientific Party, 1982). Unless fault lines and fractures in the massive sediment layers of Guaymas Basin provide suitable transport pathways (Gieskes et al., 1982), deep hydrocarbon reservoirs such as those at Sites U1545 and U1546 would remain confined to the deep subsurface and age in place after the initial "burst" of hydrocarbon production and expulsion during sill emplacement. Such reservoirs would remain distinct from very young hydrocarbons in surficial sediment samples (^{14}C age of ~6000 years) that are most likely generated by thermal maturation of organic matter in shallow subsurface sediments of Guaymas Basin, in consequence of shallow and recent sill emplacements (Peter et al., 1991).

5. Acknowledgments

This study was supported by NSF grant OCE-2046799 to VE, PM, and AT; NSF grant OCE-1829903 to VE, PM, and AT; and NASA Exobiology grant APP-0244-001 to AT. IODP Expedition 385 participants were aided by IODP cruise and postcruise support. We thank all IODP Expedition 385 scientists, technicians, drillers, and crew for making sample recovery, and by proxy, this research project possible. We gratefully acknowledge the shipboard curatorial team who kept the sediment samples and metadata organized and well-cataloged.

References

Benito Merino, D., Zehnle, H., Teske, A., and Wegener, G., 2022. Deep-branching ANME-1c archaea grow at the upper temperature limit of anaerobic oxidation of methane. Frontiers in Microbiology, 13:988871. **https://doi.org/10.3389/fmicb.2022.988871**

Berndt, C., Hensen, C., Mortera-Gutierrez, C., Sarkar, S., Geilert, S., Schmidt, M., Liebetrau, V., Kipfer, R., Scholz, F., Doll, M., Muff, S., Karstens, J., Planke, S., Petersen, S., Böttner, C., Chi, W.-C., Moser, M., Behrendt, R., Fiskal, A., Lever, M.A., Su, C.-C., Deng, L., Brennwald, M.S., and Lizarralde, D., 2016. Rifting under steam—how rift magmatism triggers methane venting from sedimentary basins. Geology, 44(9):767–770. **https://doi.org/10.1130/G38049.1**

Calvert, S.E., 1966. Origin of diatom-rich, varved sediments from the Gulf of California. The Journal of Geology, 74(5):546–565. **http://www.jstor.org/stable/30059298**

Claypool, G.E., and Kvenvolden, K.A., 1983. Methane and other hydrocarbon gases in marine sediment. Annual Review of Earth and Planetary Sciences, 11(1):299–327. **https://doi.org/10.1146/annurev.ea.11.050183.001503**

Dalzell, C.J., Todd Ventura, G., Walters, C.C., Nelson, R.K., Reddy, C.M., Seewald, J.S., and Sievert, S.M., 2021. Hydrocarbon transformations in sediments from the Cathedral Hill hydrothermal vent complex at Guaymas Basin, Gulf

of California – a chemometric study of shallow seep architecture. Organic Geochemistry, 152:104173. **https://doi.org/10.1016/j.orggeochem.2020.104173**

De la Lanza-Espino, G., and Soto, L.A., 1999. Sedimentary geochemistry of hydrothermal vents in Guaymas Basin, Gulf of California, Mexico. Applied Geochemistry, 14(4):499–510. **https://doi.org/10.1016/S0883-2927(98)00064-X**

Dowell, F., Cardman, Z., Dasarathy, S., Kellermann, M.Y., Lipp, J.S., Ruff, S.E., Biddle, J.F., McKay, L.J., MacGregor, B.J., Lloyd, K.G., Albert, D.B., Mendlovitz, H., Hinrichs, K.-U., and Teske, A., 2016. Microbial communities in methane- and short chain alkane-rich hydrothermal sediments of Guaymas Basin. Frontiers in Microbiology, 7. **https://doi.org/10.3389/fmicb.2016.00017**

Edgcomb, V.P., Teske, A.P., and Mara, P., 2022. Microbial hydrocarbon degradation in Guaymas Basin—exploring the roles and potential interactions of fungi and sulfate-reducing bacteria. Frontiers in Microbiology, 13. **https://doi.org/10.3389/fmicb.2022.831828**

Einsele, G., Gieskes, J.M., Curray, J., Moore, D.M., Aguayo, E., Aubry, M.-P., Fornari, D., Guerrero, J., Kastner, M., Kelts, K., Lyle, M., Matoba, Y., Molina-Cruz, A., Niemitz, J., Rueda, J., Saunders, A., Schrader, H., Simoneit, B., and Vacquier, V., 1980. Intrusion of basaltic sills into highly porous sediments, and resulting hydrothermal activity. Nature, 283(5746):441–445. **https://doi.org/10.1038/283441a0**

Gieskes, J.M., Kastner, M., Einsele, G., Kelts, K., and Niemitz, J., 1982. Hydrothermal activity in the Guaymas Basin, Gulf of California: a synthesis. In Curray, J.R., Moore, D.G., et al., Initial Reports of the Deep Sea Drilling Project. 64: Washington, DC (US Government Printing Office), 1159–1167. **https://doi.org/10.2973/dsdp.proc.64.155.1982**

Gilbert, D., and Summerhayes, C.P., 1982. Organic facies and hydrocarbon potential in the Gulf of California. In Curray, J.R., Moore, D.G., et al., Initial Reports of the Deep Sea Drilling Project. 64: Washington, DC (US Government Printing Office), 865–870. **https://doi.org/10.2973/dsdp.proc.64.130.1982**

Hanke, U.M., Lima-Braun, A.L., Eglinton, T.I., Donnelly, J.P., Galy, V., Poussart, P., Hughen, K., McNichol, A.P., Xu, L., and Reddy, C.M., 2019. Significance of perylene for source allocation of terrigenous organic matter in aquatic sediments. Environmental Science & Technology, 53(14):8244–8251. **https://doi.org/10.1021/acs.est.9b02344**

Head, I.M., Jones, D.M., and Larter, S.R., 2003. Biological activity in the deep subsurface and the origin of heavy oil. Nature, 426(6964):344–352. **https://doi.org/10.1038/nature02134**

Kastner, M., 1982. Evidence for two distinct hydrothermal systems in the Guaymas Basin. In Curray, J.R., Moore, D.G., et al., Initial Reports of the Deep Sea Drilling Project. 64: Washington, DC (US Government Printing Office), 1143–1157. **https://doi.org/10.2973/dsdp.proc.64.154.1982**

Kawka, O.E., and Simoneit, B.R.T., 1994. Hydrothermal pyrolysis of organic matter in Guaymas Basin: I. Comparison of hydrocarbon distributions in subsurface sediments and seabed petroleums. Organic Geochemistry, 22(6):947–978. **https://doi.org/10.1016/0146-6380(94)90031-0**

Laso-Pérez, R., Hahn, C., Vliet, D.M.v., Tegetmeyer, H.E., Schubotz, F., Smit, N.T., Pape, T., Sahling, H., Bohrmann, G., Boetius, A., Knittel, K., and Wegener, G., 2019. Anaerobic degradation of non-methane alkanes by "Candidatus Methanoliparia" in hydrocarbon seeps of the Gulf of Mexico. MBio, 10(4):10.1128/mbio.01814-01819. **https://doi.org/10.1128/mbio.01814-19**

Liang, R., Davidova, I.A., Teske, A., and Suflita, J.M., 2023. Evidence for the anaerobic biodegradation of higher molecular weight hydrocarbons in the Guaymas Basin. International Biodeterioration & Biodegradation, 181:105621. **https://doi.org/10.1016/j.ibiod.2023.105621**

Lizarralde, D., Soule, S.A., Seewald, J.S., and Proskurowski, G., 2011. Carbon release by off-axis magmatism in a young sedimented spreading centre. Nature Geoscience, 4:50–54. **https://doi.org/10.1038/ngeo1006**

Lizarralde, D., Teske, A., Höfig, T.W., González-Fernández, A., and IODP Expedition 385 Scientists, 2023. Carbon released by sill intrusion into young sediments measured through scientific drilling. Geology. **https://doi.org/10.1130/G50665.1**

Mara, P., Nelson, R.K., Reddy, C.M., Teske, A., and Edgcomb, V.P., 2022. Sterane and hopane biomarkers capture microbial transformations of complex hydrocarbons in young hydrothermal Guaymas Basin sediments. Communications Earth & Environment, 3(1):250. **https://doi.org/10.1038/s43247-022-00582-8**

Mara, P., Teske, A., and Edgcomb, V., 2024. Supplementary material, **https://doi.org/10.14379/iodp.proc.385.205supp.2024**. In Mara, P., Teske, A., and Edgcomb, V., Data report: hydrocarbon profiles of selected IODP Expedition 385 Guaymas Basin samples and comparison to shallow surficial push core samples from AT42-05. In Teske, A., Lizarralde, D., Höfig, T.W., and the Expedition 385 Scientists, Guaymas Basin Tectonics and Biosphere. Proceedings of the International Ocean Discovery Program, 385: College Station, TX (International Ocean Discovery Program).

McGenity, T.J., McKew, B.A., and Lea-Smith, D.J., 2021. Cryptic microbial hydrocarbon cycling. Nature Microbiology, 6(4):419-420. **https://doi.org/10.1038/s41564-021-00881-4**

Morono, Y., Teske, A., Galerne, C., Bojanova, D., Edgcomb, V., Meyer, N., Schubert, F., and Toffin, L., and the IODP Expedition 385 Scientists, 2022. Microbial cell distribution in the Guaymas Basin subseafloor biosphere, a young marginal rift basin with rich organics and steep temperature gradient. Presented at the EGU General Assembly, Vienna, Austria, 23–27 May 2022. **https://doi.org/10.5194/egusphere-egu22-3312**

Ondréas, H., Scalabrin, C., Fouquet, Y., and Godfroy, A., 2018. Recent high-resolution mapping of Guaymas hydrothermal fields (Southern Trough). Bulletin de la Société Géologique de France, 189(1). **https://doi.org/10.1051/bsgf/2018005**

Peter, J.M., Peltonen, P., Scott, S.D., Simoneit, B.R.T., and Kawka, O.E., 1991. ^{14}C ages of hydrothermal petroleum and carbonate in Guaymas Basin, Gulf of California: implications for oil generation, expulsion, and migration. Geology, 19(3):253–256. **https://doi.org/10.1130/0091-7613(1991)019<0253:CAOHPA>2.3.CO;2**

Ramírez, G.A., Paraskevi, V.M., Sehein, T., Wegener, G., Chambers, C.R., Joye, S.B., Peterson, R.N., Philippe, A., Burgaud, G., Edgcomb, V.P., and Teske, A.P. , 2021. Environmental factors shaping bacterial, archaeal and fungal community structure in hydrothermal sediments of Guaymas Basin, Gulf of California. PloS One. **https://doi.org/10.1371/journal.pone.0256321**

Rullkötter, J., von der Dick, H., and Welte, D.H., 1982. Organic petrography and extractable hydrocarbons of sediments from the Gulf of California, Deep Sea Drilling Project Leg 64. In Curray, J.R., Moore, D.G., et al., Initial Reports of the Deep Sea Drilling Project. 64: Washington, DC (US Government Printing Office), 837–853. **https://doi.org/10.2973/dsdp.proc.64.128.1982**

Schrader, H., 1982. Diatom biostratigraphy and laminated diatomaceous sediments from the Gulf of California, Deep Sea Drilling Project Leg 64. In Curray, J.R., Moore, D.G., et al., Initial Reports of the Deep Sea Drilling Project 64: Washington, DC (US Government Printing Office), 973–981. **https://doi.org/10.2973/dsdp.proc.64.142.1982**

Shipboard Scientific Party, 1982. Guaymas Basin: Sites 477, 478, and 481. In Curray, J.R., Moore, D.G., et al., Initial Reports of the Deep Sea Drilling Project. 64: Washington, DC (US Government Printing Office), 211–415. **https://doi.org/10.2973/dsdp.proc.64.104.1982**

Silliman, J.E., Meyers, P.A., and Eadie, B.J., 1998. Perylene: an indicator of alteration processes or precursor materials? Organic Geochemistry, 29(5):1737–1744. **https://doi.org/10.1016/S0146-6380(98)00056-4**

Simoneit, B.R.T., 1985. Hydrothermal petroleum: genesis, migration, and deposition in Guaymas Basin, Gulf of California. Canadian Journal of Earth Sciences, 22(12):1919–1929. **https://doi.org/10.1139/e85-208**

Simoneit, B.R.T., 1990. Petroleum generation, an easy and widespread process in hydrothermal systems: an overview. Applied Geochemistry, 5(1):3–15. **https://doi.org/10.1016/0883-2927(90)90031-Y**

Simoneit, B.R.T., and Bode, G.R., 1982. Appendix II: carbon/carbonate and nitrogen analyses, Leg 64, Gulf of California. In Curray, J.R., Moore, D. G., et al., Initial Reports of the Deep Sea Drilling Project. 64: Washington, DC (US Government Printing Office), 1303–1305. **https://doi.org/10.2973/dsdp.proc.64.app2.1982**

Stout, S.A., 2016. Oil spill fingerprinting method for oily matrices used in the Deepwater Horizon NRDA. Environmental Forensics, 17(3):218–243. **https://doi.org/10.1080/15275922.2016.1177759**

Teske, A., 2019. Hydrocarbon-degrading microbial communities in natural oil seeps. In McGenity, T.J., Microbial Communities Utilizing Hydrocarbons and Lipids: Members, Metagenomics and Ecophysiology. Handbook of Hydrocarbon and Lipid Microbiology. K.N. Timmis, M. Boll, O. Geiger, H. Goldfine, T. Krell, S.Y. Lee, T.J. McGenity, F. Rojo, D.Z. Sousa, A.J.M. Stams, R. Steffan, and H. Wilkes (Series Eds.): 81–111. **https://doi.org/10.1007/978-3-030-14785-3_3**

Teske, A., Lizarralde, D., Höfig, T.W., Aiello, I.W., Ash, J.L., Bojanova, D.P., Buatier, M.D., Edgcomb, V.P., Galerne, C.Y., Gontharet, S., Heuer, V.B., Jiang, S., Kars, M.A.C., Khogenkumar Singh, S., Kim, J.-H., Koornneef, L.M.T., Marsaglia, K.M., Meyer, N.R., Morono, Y., Negrete-Aranda, R., Neumann, F., Pastor, L.C., Peña-Salinas, M.E., Pérez Cruz, L.L., Ran, L., Riboulleau, A., Sarao, J.A., Schubert, F., Stock, J.M., Toffin, L.M.A.A., Xie, W., Yamanaka, T., and Zhuang, G., 2021a. Site U1545. In Teske, A., Lizarralde, D., Höfig, T.W., and the Expedition 385 Scientists, Guaymas Basin Tectonics and Biosphere. Proceedings of the International Ocean Discovery Program, 385: College Station, TX (International Ocean Discovery Program). **https://doi.org/10.14379/iodp.proc.385.103.2021**

Teske, A., Lizarralde, D., Höfig, T.W., Aiello, I.W., Ash, J.L., Bojanova, D.P., Buatier, M.D., Edgcomb, V.P., Galerne, C.Y., Gontharet, S., Heuer, V.B., Jiang, S., Kars, M.A.C., Khogenkumar Singh, S., Kim, J.-H., Koornneef, L.M.T., Marsaglia, K.M., Meyer, N.R., Morono, Y., Negrete-Aranda, R., Neumann, F., Pastor, L.C., Peña-Salinas, M.E., Pérez Cruz, L.L., Ran, L., Riboulleau, A., Sarao, J.A., Schubert, F., Stock, J.M., Toffin, L.M.A.A., Xie, W., Yamanaka, T., and Zhuang, G., 2021b. Site U1546. In Teske, A., Lizarralde, D., Höfig, T.W., and the Expedition 385 Scientists, Guaymas Basin Tectonics and Biosphere. Proceedings of the International Ocean Discovery Program, 385: College Station, TX (International Ocean Discovery Program). **https://doi.org/10.14379/iodp.proc.385.104.2021**

Teske, A., Lizarralde, D., Höfig, T.W., Aiello, I.W., Ash, J.L., Bojanova, D.P., Buatier, M.D., Edgcomb, V.P., Galerne, C.Y., Gontharet, S., Heuer, V.B., Jiang, S., Kars, M.A.C., Khogenkumar Singh, S., Kim, J.-H., Koornneef, L.M.T., Marsaglia, K.M., Meyer, N.R., Morono, Y., Negrete-Aranda, R., Neumann, F., Pastor, L.C., Peña-Salinas, M.E., Pérez Cruz, L.L., Ran, L., Riboulleau, A., Sarao, J.A., Schubert, F., Stock, J.M., Toffin, L.M.A.A., Xie, W., Yamanaka, T., and Zhuang, G., 2021c. Sites U1547 and U1548. In Teske, A., Lizarralde, D., Höfig, T.W., and the Expedition 385 Scientists, Guaymas Basin Tectonics and Biosphere. Proceedings of the International Ocean Discovery Program, 385: College Station, TX (International Ocean Discovery Program). **https://doi.org/10.14379/iodp.proc.385.105.2021**

Teske, A., Lizarralde, D., Höfig, T.W., Aiello, I.W., Ash, J.L., Bojanova, D.P., Buatier, M.D., Edgcomb, V.P., Galerne, C.Y., Gontharet, S., Heuer, V.B., Jiang, S., Kars, M.A.C., Khogenkumar Singh, S., Kim, J.-H., Koornneef, L.M.T., Marsaglia, K.M., Meyer, N.R., Morono, Y., Negrete-Aranda, R., Neumann, F., Pastor, L.C., Peña-Salinas, M.E., Pérez Cruz, L.L., Ran, L., Riboulleau, A., Sarao, J.A., Schubert, F., Stock, J.M., Toffin, L.M.A.A., Xie, W., Yamanaka, T., and Zhuang, G., 2021d. Site U1549. In Teske, A., Lizarralde, D., Höfig, T.W., and the Expedition 385 Scientists, Guaymas Basin Tectonics and Biosphere. Proceedings of the International Ocean Discovery Program, 385: College Station, TX (International Ocean Discovery Program). **https://doi.org/10.14379/iodp.proc.385.106.2021**

Teske, A., Lizarralde, D., Höfig, T.W., Aiello, I.W., Ash, J.L., Bojanova, D.P., Buatier, M.D., Edgcomb, V.P., Galerne, C.Y., Gontharet, S., Heuer, V.B., Jiang, S., Kars, M.A.C., Khogenkumar Singh, S., Kim, J.-H., Koornneef, L.M.T., Marsaglia, K.M., Meyer, N.R., Morono, Y., Negrete-Aranda, R., Neumann, F., Pastor, L.C., Peña-Salinas, M.E., Pérez Cruz, L.L., Ran, L., Riboulleau, A., Sarao, J.A., Schubert, F., Stock, J.M., Toffin, L.M.A.A., Xie, W., Yamanaka, T., and Zhuang, G., 2021e. Site U1551. In Teske, A., Lizarralde, D., Höfig, T.W., and the Expedition 385 Scientists, Guaymas Basin Tectonics and Biosphere. Proceedings of the International Ocean Discovery Program, 385: College Station, TX (International Ocean Discovery Program). **https://doi.org/10.14379/iodp.proc.385.108.2021**

Teske, A., 2024. The Guaymas Basin – a hot spot for hydrothermal generation and anaerobic microbial degradation of hydrocarbons. International Biodeterioration & Biodegradation, 186:105700. **https://doi.org/10.1016/j.ibiod.2023.105700**

Teske, A., Lizarralde, D., and Höfig, T.W., 2018. Expedition 385 Scientific Prospectus: Guaymas Basin Tectonics and Biosphere. International Ocean Discovery Program. **https://doi.org/10.14379/iodp.sp.385.2018**

Teske, A., McKay, L.J., Ravelo, A.C., Aiello, I., Mortera, C., Núñez-Useche, F., Canet, C., Chanton, J.P., Brunner, B., Hensen, C., Ramírez, G.A., Sibert, R.J., Turner, T., White, D., Chambers, C.R., Buckley, A., Joye, S.B., Soule, S.A., and Lizarralde, D., 2019. Characteristics and evolution of sill-driven off-axis hydrothermalism in Guaymas Basin – the Ringvent site. Scientific Reports, 9(1):13847. **https://doi.org/10.1038/s41598-019-50200-5**

Teske, A., Wegener, G., Chanton, J.P., White, D., MacGregor, B., Hoer, D., de Beer, D., Zhuang, G., Saxton, M.A., Joye, S.B., Lizarralde, D., Soule, S.A., and Ruff, S.E., 2021f. Microbial communities under distinct thermal and geochemical regimes in axial and off-axis sediments of Guaymas Basin. Frontiers in Microbiology, 12:633649. **https://doi.org/10.3389/fmicb.2021.633649**

Venkatesan, M.I., 1988. Occurrence and possible sources of perylene in marine sediments-a review. Marine Chemistry, 25(1):1–27. **https://doi.org/10.1016/0304-4203(88)90011-4**

Wakeham, S.G., Schaffner, C., Giger, W., Boon, J.J., and De Leeuw, J.W., 1979. Perylene in sediments from the Namibian Shelf. Geochimica et Cosmochimica Acta, 43(7):1141–1144. **https://doi.org/10.1016/0016-7037(79)90100-5**

Whelan, J.K., and Hunt, J.M., 1982. C_1–C_8 hydrocarbons in Leg 64 sediments, Gulf of California. In Curray, J.R., Moore, D.G., et al., Initial Reports of the Deep Sea Drilling Project. 64: Washington, DC (US Government Printing Office), 763–780. **https://doi.org/10.2973/dsdp.proc.64.123.1982**

Zehnle, H., Laso-Pérez, R., Lipp, J., Riedel, D., Benito Merino, D., Teske, A., and Wegener, G., 2023. Candidatus Alkanophaga archaea from Guaymas Basin hydrothermal vent sediment oxidize petroleum alkanes. Nature Microbiology, 8(7):1199–1212. **https://doi.org/10.1038/s41564-023-01400-3**